IEEE Access
Multidisciplinary ⋮ Rapid Review ⋮ Open Access Journal

Received November 25, 2021, accepted December 28, 2021, date of publication January 4, 2022, date of current version January 20, 2022.

Digital Object Identifier 10.1109/ACCESS.2022.3140340

Flow-Based Rip Current Detection and Visualization

ISSEI MORI[1], AKILA DE SILVA[1], GREGORY DUSEK[2], JAMES DAVIS[1], (Senior Member, IEEE), AND ALEX PANG[1]

[1]Computer Science and Engineering Department, University of California at Santa Cruz, Santa Cruz, CA 95064, USA
[2]NOAA National Ocean Service, Silver Spring, MD 20910, USA

Corresponding author: Issei Mori (imori@ucsc.edu)

This work was supported in part by the Southeast Coastal Ocean Observing Regional Association (SECOORA) through the National Oceanic and Atmospheric Administration (NOAA) Financial Assistance under Award NA20NOS0120220, and in part by the WISEautomotive through the Advanced Technology Center+ (ATC+) Program Award from the Korean Ministry of Trade, Industry and Energy (MOTIE).

ABSTRACT Rip currents are like rivers of fast-moving water that can quickly carry the unwary out to sea. They are not easy to recognize, especially to the untrained observer. Other than in-situ current measurements, there exists a number of methods that analyzes images and videos to detect rip currents. Most of these techniques base their detection on the appearance of rip currents such as foamy pattern, discoloration of water, and locations of breaking waves. Leading methods use either image processing or machine learning of images and/or video input. In this paper, we analyze the behavior of water movement rather than simply its appearance to detect rip currents. Specifically, we investigated several flow visualization methods and tune them to detect rip currents. Based on our study, we recommend two methods that allowed us to detect rip currents where other methods have failed. And because the methods originated as visualization techniques, any presence of rip currents are automatically highlighted. We also evaluated these two methods against previously annotated results by rip current experts, and found that our detections were sufficiently sensitive that some expert annotations were relabeled.

INDEX TERMS Feature detection, flow visualization, marine safety, time varying vector field, video analysis.

I. INTRODUCTION

Rip currents are dangerous and can be deadly. The majority of the population does not know how to identify them. Detecting rip currents in webcam video can inform users of potential hazards in near real-time and be utilized to support ongoing efforts at rip current prediction. Previously proposed methods detect some types of rip currents but not others. While image processing and machine learning methods perform well on specific types of rip currents, they are not applicable in all scenarios. This paper proposes and investigates a more general approach based on flow analysis and adapting flow visualization methods to detect rip currents.

Beaches around populated urban areas attract many beach goers and other recreational users. However, the beach can pose a grave danger to the unwary public in the form of rip currents [1]. People who unknowingly enter a rip current may be carried out to the sea if the current is strong enough. Globally there are thousands of drownings each year due to rip currents [2], [3]. It is estimated that around 82% of rescues on the beaches in the United States are due to rip currents [4]. Year-to-year statistics collected by the U.S. National Oceanic and Atmospheric Administration (NOAA) [5] indicate that there has been no significant decline in the number of drowning fatalities due to rip currents [6] despite the proliferation of signage, videos and other public safety messaging warning of the potential dangers rip currents pose.

Even people with some knowledge about beach safety can have difficulty in properly identifying rip currents. In a 2008 study, researchers found that almost 80% of surveyed Australian beach goers were aware of common rip safety advice such as "swim parallel to the beach." However, only 40% could identify a rip current when shown a picture of one, even though 80% thought they could [7]. In fact, even professional lifeguards cannot always accurately identify the presence of rip currents [4]. The reality is that rip currents are often not readily or easily identifiable to the average beach goer [8]. Furthermore, the most vulnerable

The associate editor coordinating the review of this manuscript and approving it for publication was Laxmisha Rai.

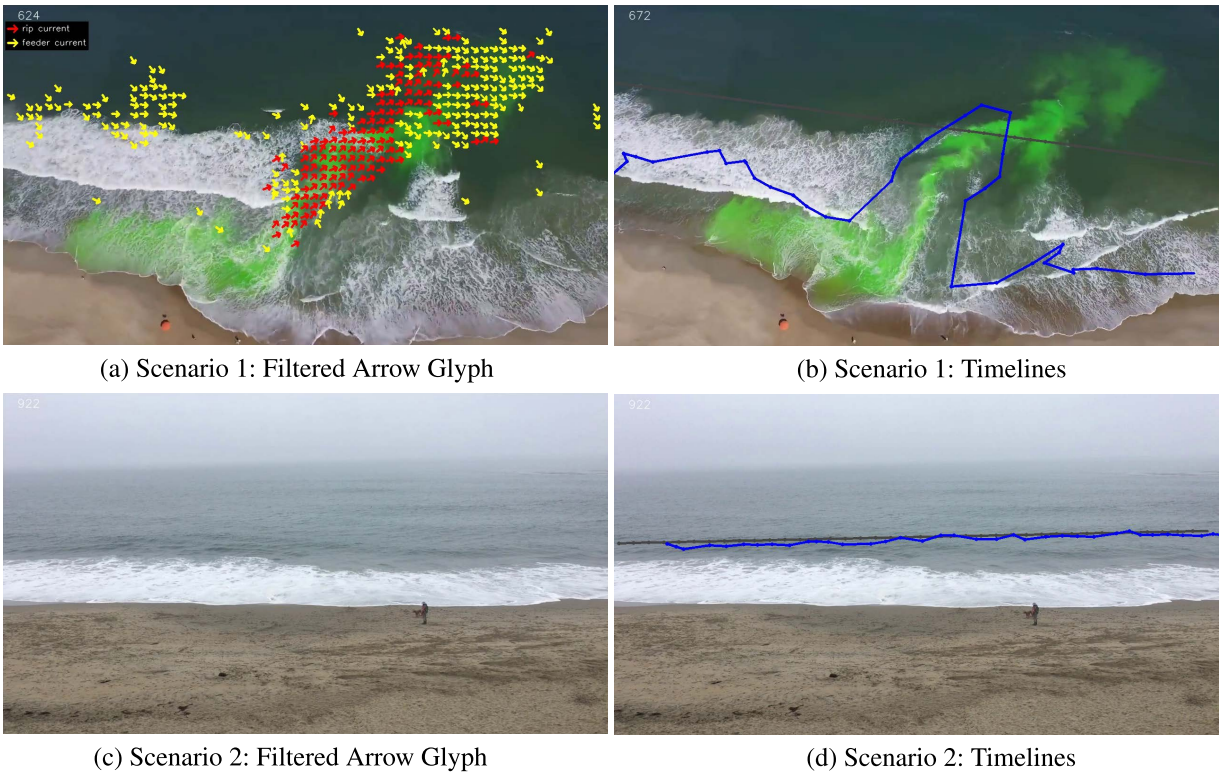

(a) Scenario 1: Filtered Arrow Glyph

(b) Scenario 1: Timelines

(c) Scenario 2: Filtered Arrow Glyph

(d) Scenario 2: Timelines

FIGURE 1. Examples of two recommended visualization methods for detecting rip currents. The filtered arrow glyph method highlights rip current and potential feeder current with arrows, and the timelines method deforms in the presence of a rip current. In Scenario 1, the original video contains green dye as a visual aid to the rip current present in the middle of the screen. The dye does not impact resulting visualizations. In (a) the filtered arrow glyph highlights the body of the rip in red and the potential feeder current in yellow. The timelines in (b) clearly shows the presence of the seaward flow caused by the rip. On the other hand, Scenario 2 shows our visualizations in the case there is no rip current. In (c), no arrows are shown, indicating that there is no rip current. In (d), the timeline is relatively straight, indicating that the flow filed is mostly uniform, hence the absence of a rip current.

ones are the occasional beach goers and weak swimmers [9]. While there are options for in-situ measurements to identify rip currents, they are generally expensive and require extensive setup. In this sense, there is currently no robust location-independent means of rip current identification.

This paper investigates the potential for using flow visualization methods as a means for identifying rip currents from short video clips. It has the potential for identifying rip currents based on the behavior of water movement rather than simply the appearance of the water state. The analysis pipeline starts with video pre-processing, including image stabilization and applying optical flow computation to obtain a time-dependent flow field. We investigate multiple flow visualization methods, including color maps, pathlines, arrow glyphs, and timelines, to detect and visualize the presence of rip currents. Examples of two of these methods on scenes with and without rip currents are shown in Figure 1. After describing the methods, we evaluate them on various data sets and compare them against other existing methods as well as human-annotated data to showcase their performance in challenging cases.

Contributions of this paper are:

- Our investigation of flow visualization methods for detecting rip currents found that standard visualization methods performed poorly when applied directly. However, with appropriate modifications driven by wave behavior, flow visualization methods can detect rip currents in scenarios where existing state-of-the-art rip detection methods fail.
- We performed comparisons between the proposed flow based methods against current best practices (classification based on Timex images) and other machine learning based methods. Our flow based methods also improved human labels that relied on Timex images alone.

II. BACKGROUND AND RELATED WORK

A. RIP CURRENTS

Rip currents are a well-studied ocean phenomenon [9]–[11]. Many factors contribute to the formation of rip currents, such as bathymetry, wave characteristics, and natural and man-made structures along the beach. As a result, there are different types of rip currents, including bathymetry-controlled rips, structural rips, circulating rips, and others [12]. Rips may either be transient, potentially moving along the beach and lasting only seconds to minutes, or persistent, holding a near-constant position for hours or days at a time. Rips that are frequently found at the same location are usually indicative of a structural feature such as jetties or piers, rocky outcrops, reefs, or persistent sandbars which lead to variations in

breaking wave heights alongshore. Regions of larger breaking waves lead to higher water levels, which then flow alongshore to regions of smaller breaking waves and lower water levels and then offshore as a rip current. On sandy beaches, regions of smaller breaking waves are often characterized by deeper channels, which are often indications of rip current presence. Rip currents may pulse, gaining strength when there is a wave set and weakening in between sets. In terms of appearance, some rips may be identified by water discoloration as beach sediment is carried by the rip past the surf zone (region where waves are breaking). In other cases, rips may be identified by a darker region of water that is flanked on either side by breaking waves. The movement of foam or other debris on the water surface can also provide clues of rip current locations. Rip currents are quite varied, dynamic, and pose a challenge to detect robustly.

B. RIP FORECASTING

Models that incorporate the dominant factors contributing to rip formation have been proposed to predict future rip current occurrence e.g. [13], [14]. In fact, NOAA recently announced an operational rip current forecast for the United States coastline [15]. Note that these models differ from efforts in this paper and other methods described in this section in that the latter focus on detection rather than forecasting. The forecast models will benefit from advances in rip detection to validate and improve rip current predictions.

C. LIFEGUARDS

Lifeguards rely on visual cues and experience to identify rips, which requires training and familiarity with the locale. However, most drownings occur on beaches without trained personnel [16], [17]. Posted signs can provide some information regarding what to do if caught in a rip current, but there is evidence that many people do not find existing signs helpful in identifying rip currents [18].

D. IN-SITU MEASUREMENTS

In-situ measurements such as acoustic doppler current profilers (ADCP), wave sensors, and acoustic velocimeters provide water column flow information [19]–[23]. However, these are expensive and challenging to deploy in the surf zone, and they only provide data for one location at a time. Fluorescein dye is commonly released into the ocean and the dispersion observed [24]–[27]. Floating drifters with embedded GPS units have also been used to measure currents [12], [28], [29]. However, these methods require some idea of where a rip might exist in the first place. They are also a research endeavor and not designed for use by the general public. In addition, they are impractical for detecting flash rips that are more transient in nature.

E. TIME-EXPOSURE IMAGES

Experts at the National Oceanic and Atmospheric Administration (NOAA) use images and video to gather statistics about rip currents [30]. These data support the validation of a rip current forecast model to alert people to potential hazards [13]. One method that has promise for visually detecting rip currents is the use of ''time exposure'' or Timex images [31]–[34]. These are obtained by simply averaging frames of a video clip, usually over a period of 10 minute intervals. This approach works well for rips that are characterized by a darker region of water flanked by breaking waves since places with consistent breaking waves will appear blurred white, while the location of a rip will appear darker. However, its main weakness is that it can only identify rips with these visual characteristics. Furthermore, because the time-averaging window is over many wave periods, it may lead to an incorrect classification e.g. for non-stationary rip currents. While Timex images are most commonly viewed by human experts, Maryan *et al.* [35] trained a machine learning model to determine whether a Timex image contains a rip channel or not. They reported a detection rate of 85% for various beach locations. Nelko also used time-averaged images and noted that prediction schemes developed at one beach location might not be directly applicable to another [36]. Nonetheless, the main weakness of any methods which rely on Timex images is their limitations on the type of rips they can identify – limited to bathymetry-controlled rips.

F. SEGMENTATION

Another method for detecting rip currents is to find discoloration due to sediment transport. Liu and Wu [23] reported that imagery captured from a stationary webcam can be segmented based on hue. Possible rips are identified if the sediment plume extends beyond some distance from the shoreline. Together with environmental monitoring equipment for wind speed, wind direction, wave height, and wave period, they have an automated system that issues alerts of flash rip dangers to beach goers. However, this method is specific to only certain locales with sediment plumes, and as with Timex images, limited to rips that exhibit sediment plumes.

G. NEURAL NETWORKS

De Silva *et al.* [37] trained a neural network model to identify rip currents from a sequence of images. They reported a detection rate of 98.4% for their test set consisting of videos with and without rip currents. However, their model can only detect rips with consistent breaking waves since they use single-frame, RGB-based images of rip currents characterized by a gap in breaking waves to train their model. Like the approaches based on Timex, their implementation is currently limited to bathymetry-controlled rips until training data are collected for other types of rips and their model retrained.

H. OPTICAL FLOW

Dense optical flow [38], [39] can be used to detect rip currents in a video. This method is attractive since optical flow fields can be directly compared against ground truth flow fields obtained from in-situ measurements [40]. Philip and Pang [41] identified rip currents by looking at the distribution

of detected flow velocities which might include motions due to wave action, possible rip, and motion in the background scenery. They assumed the rip current to be in a *single* seaward direction, with rip regions above a certain velocity threshold and region size. Unfortunately, rip currents do not necessarily flow in a straight line, leading to false-negative results. Also, rip currents often have feeder currents that travel alongshore, bringing water that feeds the rip current's main body. The work reported in this paper builds upon [41] to detect nonlinear rip currents and feeder currents, and also include comparisons with alternative detection methods.

More recently, Anderson *et al.* [42] introduced WAMFlow (wave-average movies) where they pre-filter the video source prior to obtaining the optical flow field. The pre-filtering aims to remove the dominant signal due to incident waves while leaving the signal due to foam or water turbidity features that might indicate the presence of rip currents and non-stationary circulation cells. In contrast, the work presented here applies the filtering on the optical flow field derived from raw video, while achieving real-time processing for the proposed pipeline. Furthermore, the focus of this paper is on adapting flow visualization methods to detect and visualize the presence of rip currents.

III. DATA AND PRE-PROCESSING

A. DATA SETS

The data set used for our investigation is composed of 27 video clips collected from the web, photographed by the authors, or obtained from collaborators. The collection includes cases with rip currents, no rip currents, and possible weak rip currents. Those that contain rip currents include different types of rips: rips with curvature, sediment plume, a dark channel between breaking waves, and structural rips. The data set also contains cases with swash (water movement on the shallow part of the beach after a wave has broken all the way to the high water mark where a wave can run up the beach) and reflection waves (or backwash off a rocky shoreline). We exclude some video from consideration because they are not suitable for flow-based analyses e.g. unstable/shaky video, contains camera pans/rotations, poor video quality e.g. blurry, duration is too short for time averaging. The videos ranged in size from 320×400 to 1920×1080, and ranged in length from 11 seconds to 60 seconds, recorded at 30 fps. In this paper we downsampled large videos to 720-pixels height and the corresponding width to keep their aspect ratio.

B. DATA REQUIREMENTS

In an ideal scenario, the video is taken from a stabilized mount, at as high an elevation as possible, with some beach in the foreground, on a sunny day, with sufficient duration and resolution. Webcams around the world, especially surf cams where there is a higher chance of finding rip currents, offer a rich potential for videos. However, most of them are not configured for rip current detection.

Flow analysis requires sufficient pixels imaging the rip current. With the settings of the optical flow method we used, the minimal width of rip current that the estimated flow field can correctly represent was roughly 80 pixels. For most of the videos obtained from a webcam that is sufficiently close to the beach, we found that image resolution of at least 640×480 is required. When the relevant section of the ocean uses only a small part of the frame, increased resolution is needed. The increased resolution does increase the computational requirements. Therefore, videos that are larger than 1080×720 are either scaled down to a height of 720 while maintaining the aspect ratio, or cropped to the region of interest.

The camera should be steady or fixed and not contain panning, rotations, zooms since frame to frame correspondence is needed to obtain the optical flow field. Small camera vibrations or drifts can be compensated by video stabilization, but excessive shaking will also make the video unsuitable.

Sufficient duration is needed to observe a rip current, usually at least one minute or at least three wave periods. The justification is that rip speed is related to breaking wave height, which in turn varies with infra-gravity wave motion, commonly called wave "sets". A wave set typically varies on the order of minutes, and we find that around one minute of video is sufficient. However, a longer video would be preferable especially for longer period waves.

C. VIDEO PRE-PROCESSING

Video must be stabilized prior to extracting the optical flow field. Videos sources from webcams can omit this step, while videos from drone or hand-held cameras can benefit from this step. Optical flow estimates motion based on differences of local neighborhood pixel values in consecutive video frames, and camera motion will produce a confounding flow field. Many video stabilization methods exist [43], [44] [45], [46], and robust automatic stabilization is possible. In this work, we simply use the Warp Stabilizer feature of Adobe After Effects. The Warp Stabilizer tracks selected static objects in the scene (e.g. a pier, rocks) and stabilizes the video using them as fiducials. We supplement with manual adjustment as needed, typically when the video contains insufficient rigid landmarks.

IV. FLOW-BASED ANALYSIS

In this paper, flow-based analysis refers to the analysis and visualization of a vector field derived from optical flow of video clips, with the goal of finding rip currents. We investigate Color Maps and Pathlines as standard baseline flow visualization methods and find them lacking. We then investigate the enhanced methods of Filtered Arrow Glyphs and Timelines and find that they perform well.

A. OPTICAL FLOW MAP

Optical flow map refers to the velocity of pixels in an image derived from motion of neighboring pixels in consecutive frames from a video. Several optical flow algorithms and surveys exist [47], [48] [49], [50], and produce a flow field

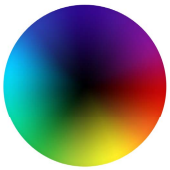

FIGURE 2. The color wheel used to map flow vector to color. The flow directions are mapped to hues, while the relative magnitudes are mapped to value (darker indicating smaller magnitudes). For example, red indicates a flow towards the right.

describing where each pixel moves from one frame to the next. Our implementation uses the OpenCV library [51] for computation. Dense optical flow is calculated at every pixel using Farneback's method [47], and used for visualizations methods that require it, such as pseudo-coloring and flow difference. To save computational cost, sparse optical flow is calculated using Lucas-Kanade [48], and used as input to the remainder of the visualization methods.

B. BASELINE VISUALIZATION METHODS

1) COLOR MAP

The most basic method of visualizing a scalar field is pseudo-coloring or color mapping. In the case of a vector field such as the vector field obtained from the optical flow across frames in a video, direction and magnitudes are mapped separately to different color properties. Specifically, we use an HSV color model where flow direction is mapped to hue (what is normally referred to as color), while flow magnitude is mapped to value (brighter or darker shade of the color). Saturation is set to one. Figure 2 shows the color wheel that we use to map the flow direction and magnitude to hue (color) and value (darker towards the center of the color wheel) respectively. For example, brighter red indicates a strong flow towards the right, while a darker red indicates a weaker flow towards the right.

Color mapping vector fields involve first converting vector information from Cartesian to polar coordinates to obtain angles and magnitudes from the 2D vector components. The magnitudes are normalized so that they range from 0.1. Angles are then mapped to hue while normalized magnitudes are mapped linearly to value. In Figure 3, the green fluorescent dye on the left image indicates the location of the rip current. On the right, is the corresponding color mapped image. The bright green regions on the right indicate a strong flow direction towards the bottom left of the image. The darker regions of the right image correspond to regions with weak to no movement. Notice that these regions correspond to the beach and areas past the surf zone, as well as the rip itself. Since the video has been stabilized, the darker color where the rip is located indicates that the speed of the rip away from shore is relatively slow compared to the speed of breaking waves as they progress toward the coastline. While this visualization allowed us to see velocity information, it was confusing to general viewers and is not usable by itself for alerting viewers to the presence of rip currents.

2) PATHLINES

Pathlines record the trajectory of a massless particle in a time-varying vector field [52]. The optical flow field derived from video analysis is a time-varying vector field $\vec{v}(\vec{p}, t)$ where the velocity $\vec{v}$ is known for each location $\vec{p}$ at time t. The pathline is obtained by integrating $\frac{d\vec{p}}{dt} = \vec{v}(\vec{p}, t)$ We use an explicit fixed step 4th order Runge-Kutta integration. If a seed point is placed in the vicinity of a rip current, we expect it to be drawn into the rip, and leave a trace of its path from the seed point towards the rip in the process. On the other hand, those seeded outside a rip zone would not be affected and would likely just be washed ashore by the incoming surf. Aside from the trajectory itself, a pathline can be colored to show some other properties such as: (a) age of the particle, which is useful to see if the trajectory is progressing seaward or not; (b) length of trajectory, which is useful to gauge relative speeds; and (c) distance from starting point, which is useful to see if a particle takes a circuitous/cyclic path or a more direct route.

To test this method, we seeded a regularly spaced 9×9 sampling grid. Figure 4 shows the 81 pathlines. Pathlines are colored by age, starting with red and getting cooler over time. Unlike Figure 3, this figure shows the cumulative effects of the flow field on the 81 seed particles, rather than an instantaneous snapshot of where the 81 particles are located. Here, we see that the trajectories are erratic (even after video stabilization). Nevertheless, one can see that pathlines are

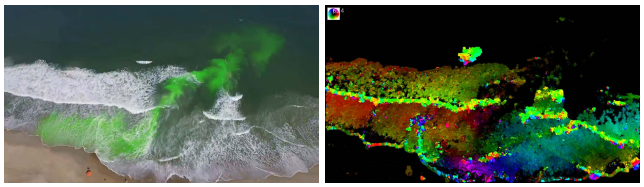

(a) Original Frame (b) Single Frame Color Map

FIGURE 3. The original frame with a rip current is shown in (a), and the corresponding single frame color map is shown in (b). Notice that the rip current traced using the green dye in (a) corresponds to the dark spot in the center of the color map in (b). Usually, rip currents are much slower than incoming waves, and its relatively weak signals are not easily observed in a single frame color map. This baseline visualization method is difficult to interpret and thus not directly usable.

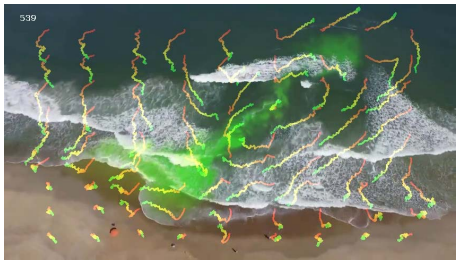

FIGURE 4. A visualization of the flow field obtained by optical flow is shown using the baseline method of pathlines. While they somewhat capture the signal of rip currents, the visualizations are not very clear.

indeed headed out in the rip, and even further beyond the outer boundary of the green tracer dye. For this method to be a rip detector, one would have to filter out the pathlines that are not in the rip. However, we cannot simply remove pathlines that are seaward, assuming one knows which direction is seaward in any given video source, because of the erratic trajectories but more importantly rips may have a circulating pattern. Because of these reasons, coupled with the clutter evident even with just a few pathines, we do not investigate this further as a detection method.

C. MODIFIED VISUALIZATION METHODS

Straightforward application of visualization methods such as the two mentioned in the previous section cannot detect rip currents. Here, we describe how domain knowledge coupled with modifications to visualization methods are necessary to arrive at effective detection and visualization of rips.

1) FILTERED ARROW GLYPHS

This is an extension of an arrow plot where an arrow is present only when a potential rip current is detected. Feeder currents that can bring material into the main rip are also included. An example of this method is shown in Figure 1 (a). Because glyphs can quickly clutter the display, we need to balance the amount of information versus the amount of clutter. Here, each frame is represented by a grid of velocities with 20-pixel spacing to ensure sufficient representation of the flow field. The idea is to alert the user to areas that might potentially be dangerous while leaving the rest of the imagery untouched.

The optical flow map detects movements across frames. Movements of clouds as well as people or pets walking on the beach are also detected. Such movements are irrelevant to rip detection so we apply a mask to ignore sky and beach regions while passing the ocean region for further processing. Because of the nature of wave motion where the predominantly observed motion is that of the incoming waves, we found that there was insufficient signal to detect rips when analyzing the flow field on individual frames. To remedy, we construct a time-averaged vector field over three wave periods. In conditions where the sea state can induce rip currents this ranges from 15-45 seconds and covers short period wind chops to longer period swells. The motivation for time-averaging is that while water may get pushed in with each wave, they also recede back to the ocean. However, the region where a rip current is situated often times have less breaking waves and hence the outward flow from a rip is more persistent and easier to detect from the time-averaged flow field.

Figure 5 shows the time-averaged flow fields for the duration of 1 and 3 wave periods. The scene contains a rip current that flows from the left and to the upper right. The corresponding color maps, described earlier, of the time-averaged flow field highlights this rip current in purple, indicating its direction. In this figure, the primary focus is to highlight flow direction and not on flow magnitude. Hence, we temporarily set all the magnitudes to 1. Notice that the color map of the one wave period averaging has another purple region in the right bottom corner of the surf zone. These false positives can be caused by transient receding water in swash zones. However, with the three wave period averaging, the false positive disappears.

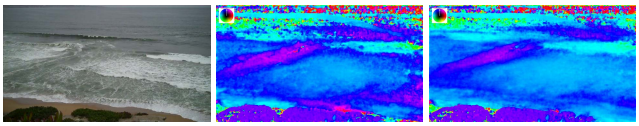

(a) Original frame (b) 1 wave period (c) 3 wave periods

FIGURE 5. Comparison of the averaged flow field color map for the duration of 1 and 3 wave periods. Original frame is shown in (a). Images in (b) and (c) are the color map of the obtained flow field, where direction is mapped to hue. In (b) and (c), the purple regions on the left correspond to rip current, indicating that there is a seaward directional flow there. Notice that the false positive in the right bottom corner disappears after averaging for 3 wave period.

Simply displaying all directional arrows produces a cluttered and confusing image. It is necessary to filter the data so that only the relevant information is shown i.e. the regions of a rip current. To achieve this, once the time-averaged vector field is constructed at each arrow position, all arrows are grouped into six bins, each representing a range of 60 degrees. The bin with the highest frequency represents the predominant flow direction, which we assume to be that of the incoming waves. The opposite direction is then assumed to be the rip direction. Vectors in this bin are represented by red arrows, while vectors in the neighboring bins on either side are represented by yellow arrows. The yellow arrows can potentially show feeder currents. They are also useful when the rip current direction extends beyond the bin that represents the rip direction e.g. for rips with high curvatures. In short, filtered arrow glyphs involve both masking out regions of a frame that is not part of the body of water, and only displaying arrow glyphs of time averaged vectors that are in the rip and feeder directions.

While this assumption of reverse flow in a rip current is simplistic, cases where the rip is quite obvious can be highlighted using this technique as in Figure 1 (a). Notice that the region with rip current is obviously marked, in contrast to Figure 1 (c) showing an ocean scene with no rip current, and no annotation.

A caveat of this method is that the direction of some rips are not necessarily opposite the incoming wave direction e.g. when waves arrive at an oblique angle to the shoreline, the rip may be as little as 90 degrees from the predominant wave direction. To be able to visualize such cases and any potential feeder current, we experimentally chose 6 bins. With 8 bins, feeder currents tend to be ignored more often, and with 4 bins, it produces much more false positives.

The filtered color map, such as the ones shown in Figure 6(b) and (e), is generated in a similar fashion as the filtered arrow glyph. Rip direction and feeder current directions are first determined using the grid of velocities with 20-pixel spacing and the binning strategy. The optical flow for

all pixels is computed, time-averaged, and mapped to color as described in section IV-B1. Parts of the color map image is then masked out if they are not in the rip or feeder current directions. Finally, this image is blended with the corresponding frame of the video. Note that regions with lower flow magnitude (low value) will contribute correspondingly less color to the blended image.

2) TIMELINES

Timelines is another flow visualization technique for analyzing time-varying flow fields. An example of this method is shown in Figure 1 (b) In the context of rip current detection, it represents a chain of virtual buoys tethered together by a massless and stretchable rope. When placed in the surf zone close to and along the shoreline, we would expect virtual buoys in the rip to be pulled out to sea, and those nearby will be pulled by feeder currents towards the main rip and eventually out to sea. The rest of the virtual buoys will likely be washed ashore. We introduce a new timeline in the surf zone every 30 seconds in order to track any new currents that may lead to the identification of pulsing rip currents. Virtual buoys along the timeline are initially spaced out at regular intervals. Over time, the relative spacing between adjacent buoys provide additional information if there is a large velocity gradient. Figure 1 (b) illustrates a case where a rip is detected. The timeline is clearly deformed and extends out along the rip channel. Contrast this with Figure 1 (d) for which no rip current is present and therefore the timeline is relatively undeformed. A grey line indicates the initial placement of the timeline in both cases. When waves are pronounced and the incident angle of the waves is perpendicular to the shoreline, the optimal placement of the timeline is parallel to the beach and in the middle of the surf zone because the rip current direction will likely have a direct seaward heading. However, when waves are weak or the incident angle of the waves is oblique to the shoreline, the rip current direction may not be directly seaward but also at an oblique angle. In such cases, we place an additional timeline perpendicular to the shoreline to better see rips that may form at an angle from the shoreline.

The process of calculating and generating the timeline is similar to that of pathline tracing. Each virtual buoy on a timeline is treated as a seed point of a pathline and its trajectory is calculated using RK4 integration. However, rather than tracing the evolution of each seed point independently, a timeline is drawn by connecting the points from all the virtual buoys, in the same order, to form a curve. As time progresses, the timeline is thus animated.

How fast a timeline moves depend on the local flow velocity. A fast moving wave could potentially push a timeline all the way to the shoreline. Such large displacements are not conducive to detecting rip currents. Simply reducing the integration step size will just increase computation cost without addressing the underlying problem. Just as we saw in Figure 5, averaging the flow field for at least three wave periods is crucial. Therefore, the timelines need to move slower than the actual speed of the waves to allow extraction of rip currents. For this reason, we multiply the optical flow field in each frame by an adjustment factor α. The α is calculated as $\alpha = d/(\delta \cdot f)$. d is the pixel-wise distance between the initial placement of the timeline and the shoreline, δ is the pixel-wise velocity of the incoming waves, and f is the total number of frames. For the videos that are longer than three minutes, we cap f to the number of frames that corresponds to three minutes in order to correctly capture transient rips. With the adjustment factor α, the timeline reaches the shoreline at the end of the specified number of frames. These slower moving timelines provide stable results.

V. RESULTS

In this section, we first evaluate the two modified flow visualization/detection methods, and then compare their performance against other methods from literature.

A. EVALUATION OF PROPOSED METHODS

We tested the two modified methods on different data set including visually obvious cases containing strong rip currents, a rip with sediment plume, and less visually apparent cases with weaker rip currents. We then applied the both methods on human labelled data set to confirm or challenge previously annotated results by rip current experts.

1) STRONG RIP CURRENTS

Figure 6 shows two examples of strong rip currents of the type that prior methods can also detect. The filtered arrow glyph visualizations in (a) and (d) are consistent in showing regions of flow against the predominant incoming wave direction. The arrows in the neighboring bins are also displayed in yellow, showing how water may feed in and out of the rip.

As noted in section IV-B, applying color maps on the flow field on a per frame basis does not help in detecting rips. We modified that method in a similar fashion as the filtered arrow glyphs, by time-averaging prior to color mapping, then filtering out non-interesting regions. This modification is illustrated in Figure 6(b) and (e). Rip currents can also be seen in one quick glance. It does require one to look at the color wheel to confirm the flow direction, whereas this step is not necessary with the filtered arrow glyph. Hence, we omit this method from further consideration.

The timeline visualizations in (c) and (f) also succeeded at showing the rip based on their protrusion or deformation. The astute reader may notice that the timeline protrusion in (f), as well as the position of the arrow glyphs and colored regions in (d) and (e) are on the right region of the darker channel in the surf zone, this indicates the region within the rip zone with strongest velocities.

2) SEDIMENT PLUMES

Figure 7 shows an example of a rip where the predominant visual signature is an obvious sediment plume. The filtered arrow glyph and the filtered color map clearly show the seaward flow caused by the strong rip. Furthermore, feeder currents from both sides of the rip are highlighted when

(a) Scene 1: Filtered Arrow Glyph (b) Scene 1: Filtered Color Map (c) Scene 1: Timelines

(d) Scene 2: Filtered Arrow Glyph (e) Scene 2: Filtered Color Map (f) Scene 2: Timelines

FIGURE 6. These evaluation videos show a prominent rip which can be easily seen on the left side of the frame in Scene 1 and on the center of the frame in Scene 2. In both scenes, all visualization methods clearly show where rip current is located. In (a), the arrows covers the body of the rip. In (b), the rip is highlighted in pink, indicating its direction. There is another region to the right where the flow direction is close to that of the rip direction and is highlighted in yellow. However, we can safely rule this out as it's not connected to the main rip and is mainly alongshore. The rip is also highlighted by the single timeline in (c). The gray line indicates the initial position of the timeline. In (d) and (e), the rip current is highlighted in the center of the frame. The region on the right side of the frame with lower right directional flow indicates this rip may circles back to the shore. (f) shows that the rip is highlighted by the single timeline.

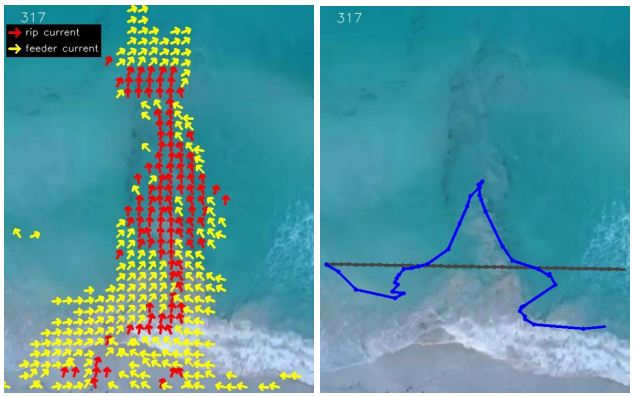

(a) Filtered Arrow Glyph (b) Timelines

FIGURE 7. This example showcases a rip with no breaking waves but which has a sediment plume. The existing machine learning methods fail in this type of data sets where there is no breaking wave features that they used for training their models. However, the optical flow methods perform well on this data set. The filtered arrow glyphs show there is a strong and obvious rip in the center. The feeder current on the both sides of the rip is also highlighted, providing additional information of the rip. The deformation of the timeline coincides well with the rip channel.

this method is applied. Swimmers in a feeder current may eventually end up in a rip and swept away. Therefore, it is crucial to visualize these regions as well.

3) WEAK RIP CURRENTS

Figure 8 shows a harder case. Even though the visual signature indicates an obvious rip where one sees the darker channel between breaking waves, the velocities are quite low.

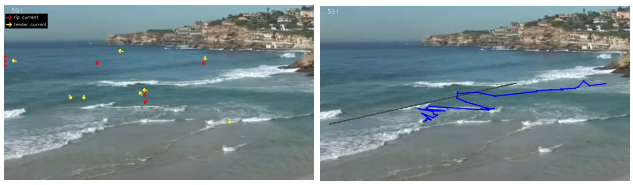

(a) Filtered Arrow Glyph (b) Timelines

FIGURE 8. This example showcases the performance of the timeline method when the flow in the rip is weak. Due to the lack of wave textures in the rip region as well as the quality of the video, the optical flow method detected very low velocity in the leftward flowing rip. We can only see a few arrow glyphs since most of them were filtered out. However, in (b), the ability of timelines to capture cumulative movement effects shows a deformation. While most of the timeline has washed in past the gray line, the deformation of the timeline in the darker region indicates a rip, albeit pretty weak and not exceeding much past the original gray line.

Hence, Figure 8(a) and Figure 8(b) do not provide much indication of a rip current. The slight differences in velocities at the rip channel and the other incoming wave regions are however enough to deform the timeline, indicating the presence of the rip at the center of the frame. The timeline method is more sensitive because it can accumulate the small deformations from weak velocities.

Figure 9 showcases another difficult case with no obvious surf zone and just shore break. In this scenario, the placement of an additional timeline perpendicular to the shoreline is helpful in visualizing the signal of a rip current that was present. Here, the deformation of the blue timeline indicates a stronger longshore component compared to the green timeline showing seaward component.

FIGURE 9. This example shows a rip that is not detectable using filtered arrow glyphs nor filtered color maps (and therefore omitted). We do see an seaward movement of the green timeline that is placed parallel to shore, but do not see any deformation to indicate a particular region that may be moving out faster than the rest. Placing another timeline, colored blue, perpendicular to shore, we can see a more pronounced deformation indicating a strong longshore current.

B. COMPARISON WITH HUMAN LABELLED DATA SET

Rip current researchers at NOAA have approximately a year's worth of labelled Timex images (from 10 minute video segments) collected from the 40th Street Miami Beach webcam. This particular webcam is part of a larger network of webcams (SECOORA) for coastal monitoring which includes beach erosion and rip current forecasting [53].

Each Timex image represents a 10 minute video segment, and were labelled by human experts as `definite yes`, `maybe yes`, `maybe no`, and `definite no` with regards to the presence of rip currents. Figure 10 shows typical views from this webcam. We note a few positive and negative aspects about this particular data set. There is minimal camera movement since the camera is on a fixed mount. Camera placement is pretty high but has a wide view. While the wide field of view is good for monitoring coastal erosion, it is less than ideal for monitoring rip currents. About 70% of the frame contains non-interesting parts i.e. sky, vegetation, sandy beach. Furthermore, due to the severe perspective distortion, only the portion of the water closest to the camera have sufficient spatial resolution (distance/pixel) to obtain a meaningful optical flow field. The camera aside, the Miami beach itself is a long sandy beach with a shallow gradual sloping bottom which does not lead to large breaking waves and is geographically protected from large swells by the Bahamas. Hence, the rip currents that do form here are typically weak.

We applied the two modified techniques (filtered arrow glyphs and timelines) on the 10 minute video clips for a random sample of labelled Timex data set. We quickly dismissed the utility of the filtered arrow glyphs and filtered color maps for this data set because of the distant camera set up which made the velocities very low. Coupled with the relatively slow wave propagation, this meant little changes in neighboring pixel values and therefore decreased signal to noise. However, because the displacement of timelines captures the *cumulative effects* of the flow field, even those from weaker rips, we were able to confirm the human labels on most of the cases that we looked at. We did find instances, such as those shown in Figure 10, where the timelines suggest a different label than the human labels. We presented these

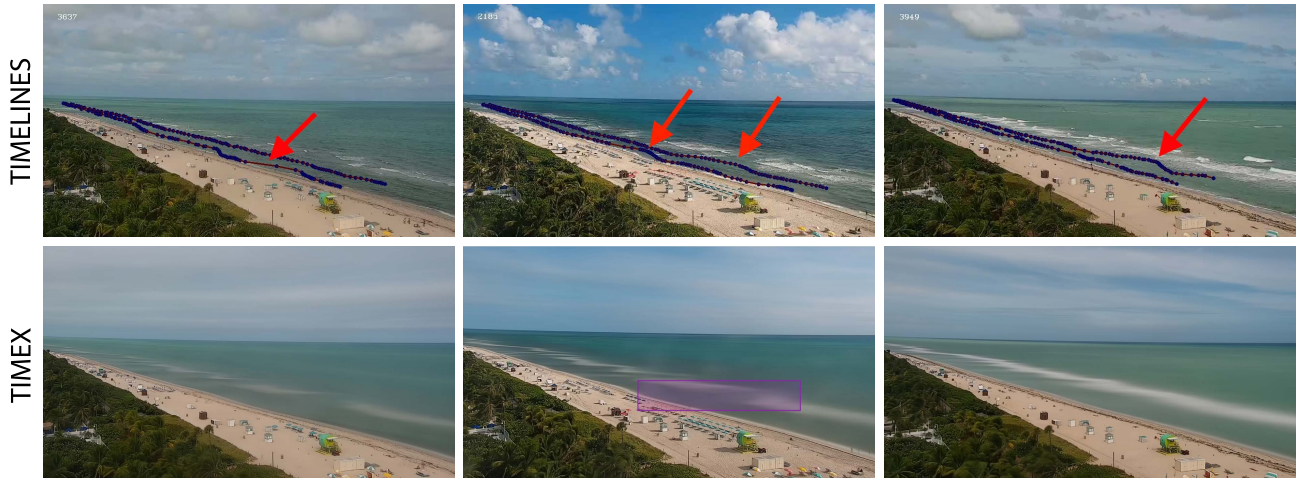

(a) Original: Maybe yes (b) Original: Definite yes (c) Original: Definite No

FIGURE 10. A comparison of *timeline* visualization with *Timex* images commonly used for human labelling. The top row shows timelines. A new timeline was released in the surf zone every 10 seconds and tracked for the next 20 seconds. In general, timelines were pushed onto the shore by incoming waves except for regions of potential rips. The bottom row shows Timex. In example (a), the Timex was originally labelled as `Maybe yes` to contain rip currents but after consulting our visualization and the complete video, the label was changed to `Maybe no`. Note that this frame of the video did show some changes in spacing of the points along the first timeline. It indicated velocity changes running parallel to the beach or a longshore current. This behavior would not have been detected using the Timex image since it was inside the region of breaking waves and not visually apparent. In example (b), the label was changed from `Definite yes` to `Maybe yes`. There were slight bumps noticeable on both timelines but not considered significant. These slight bumps indicated possibly some weak rip currents. In example (c), the label was revised dramatically from `Definite no` to `Definite yes`. The second timeline showed a fairly significant bump showing where the rip was located. Examples (a) and (b) both had the Timex characteristic darker region in between lighter regions of breaking waves. In (c) the Timex darker region was not present due to stronger surf conditions during that period, which was why the initial human label relying only on the Timex gave incorrect labels.

(a) Rip detection using Timex of Figure 1(row 1). (b) Rip detection using Timex of Figure 6(row 1).

FIGURE 11. Two examples where rip detection using timex images failed even when the visual signature of the rips are very strong.

to the experts who originally labelled the data set and asked them to view the video associated with the Timex images to make a more careful determination. In these instances, the experts changed their labels after reviewing the video. Note that the label of `maybe yes` seem to be used for cases where the rip is considered weak or the rip signal is not conclusive.

While rip detection using Timex images is less time consuming than watching video clips, and the signature pattern of rip currents in Timex images are easier to discern than looking at raw video by humans, solely relying on them can lead to incorrect classifications. Our small study demonstrates the utility of timelines for more accurate labelling compared to Timex images alone. The human experts indicated that the visualizations were valuable and contained cues which did not exist in Timex visualizations. For study locations with fixed camera mounts, accompanying Timex images with our visualization output can help improve labelling accuracy. This is an important process in collecting good training data for building automated classification models using machine learning methods such as those reported in [35], [37].

C. COMPARISON ACROSS METHODS

We compared how the different published methods detected rip currents in the video clips shown in Figures 1, 6, 7, 8, 9, and 10. The following video clips contain rip currents: Figures 1(row 1), 6, 7, 8, 9, 10(column b), and 10(column c). The following video clips do not contain rips: Figures 1(row 2) and 10(column a). Table 1 summarizes the results. A *yes* entry means the method correctly detected the rip if present (true positive), or correctly marked the video as not containing a rip (true negative). A *no* entry means the method gave a false positive or false negative result.

1) COMPARISON WITH MACHINE LEARNING METHODS

Currently, there are two rip detection methods that utilize machine learning methods. Maryan *et al.* [35] employ a Viola-Jones framework [54] to train their model to detect rips from Timex images (see Timex column in Table 1), while de Silva *et al.* [37] used a modified deep learning technique Faster RCNN [55] with an accumulation buffer to aggregate frames across time to improve prediction. That model was trained to detect rips from images and video clips (see the Faster RCNN column in Table 1). Rip detection that relies on Timex images are inherently limited to bathymetry controlled rips where the visual signature is a darker channel in between breaking waves. The model described in [37] is also limited to bathymetry controlled rips. However, that limitation is not inherent to the deep learning technique they used but rather the training data they used to train their model. Given these considerations, we would expect both detectors to do well in detecting bathymetry controlled rips and not well with other types of rips.

The Timex and Faster RCNN columns in Table 1 show how the machine learning methods fare in classifying and detecting rip currents. Our expectation is that Timex should perform well on all but Figures 7 (sediment plume) and 9

TABLE 1. Comparison of filtered color maps, filtered arrow glyphs, and timeline methods against other published methods that analyze images and/or videos. A *yes* indicates a (mostly) correct detection. The last row indicates the ratio of # correct to total. Notice that none of the existing methods is able to provide correct detections in all of the videos. In contrast timelines provides correct detections in all eight videos.

	Video Clip	Timex [35]	Faster RCNN [37]	Optical Flow [41]	Image Processing [23]	Filtered Color Map [Ours]	Filtered Arrow Glyph [Ours]	Timeline [Ours]
Figure 1(1)	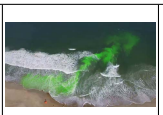	*no*	*yes*	*yes*	*no*	*yes*	*yes*	*yes*
Figure 1(2)		*no*	*yes*	*yes*	*no*	*yes*	*yes*	*yes*
Figure 6(1)		*yes*	*yes*	*no*	*no*	*yes*	*yes*	*yes*
Figure 6(2)	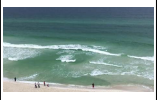	*no*	*yes*	*yes*	*no*	*yes*	*yes*	*yes*
Figure 7		*no*	*no*	*yes*	*yes*	*yes*	*yes*	*yes*
Figure 8		*no*	*yes*	*no*	*no*	*no*	*no*	*yes*
Figure 9		*no*	*no*	*no*	*no*	*no*	*no*	*yes*
Figure 10		*no*	*no*	*no*	*no*	*no*	*no*	*yes*
	Ratio	1/8	5/8	4/8	1/8	5/8	5/8	8/8

(no visual signature). Looking at the actual tests, we see that Timex performed poorly. Figure 11 shows two rips with strong visual signatures where the method based on Timex images failed. When we reran the data but fed individual frames to the model that learned to classify Timex images, the results improved slightly. There were 69% of the frames from Figure 6(1) that were correctly labelled. Hence, we marked Figure 6(1) as a *yes* in the Timex column.

2) COMPARISON WITH PREVIOUS FLOW BASED METHOD

The flow-based method described in [41] also analyzed the optical flow field derived from the video. However, it did not account for wave pulsing and used simple statistics to guess the seaward rip direction. While this may work in the typical bathymetry controlled rips, the assumption that rip direction is always straight also makes this method less flexible. Furthermore, the visualization of the detected rip is a simple reddish region to warn presence of rip and does not impart any velocity information. Figure 12 shows the output of this method on the data set shown in Figure 6(2). The highlighted regions corresponds well with the red arrows in Figure 6(d) and the pink regions in Figure 6(e). Somewhat surprising, it failed on both Figure 6(1) and Figure 8. Upon reviewing those two videos, the speed of the rip is very slow. So, even while there are strong visual cues in both cases, the per frame velocities at the rip regions were low and appeared spurious and therefore did not pass the threshold set by the method. This method also failed in Figures 9 and 10. As mentioned earlier, the velocities in Figure 9 are also very low and per frame velocity analyses fail. In Figure 10, because the camera is so far away, each pixel covers a much larger area and therefore less sensitive to velocity changes.

FIGURE 12. The same frame as Figure 6(2) but using the method from [41].

3) COMPARISON WITH IMAGE PROCESSING METHOD

The image processing method for rip detection described in [23] detects transient rips in video feeds from a fixed webcam. Rips at this location are characterized by discoloration in the water that extends some distance from shore. Based on the camera orientation, the authors rectified the frames and set a threshold line some distance from shore where any discoloration beyond that line is considered a rip. Given that this method is designed to detect rips with sediment plumes, we expect that it should do well with Figure 7, assuming that a threshold line has been set up as well. Indeed, this is what we observe with this approach in Table 1. However, this method is specialize to detect only this type of rip and does not detect other types of rips.

We provide Table 1 summarizing the performance of our methods and published methods on the 8 rip current videos shown in this paper. We find that the published methods are each limited to a specific class of rip currents and none of the existing methods are able to correctly label all videos. In contrast, all of the flow based visualization methods work at least as well as the best alternate method, and Timelines in particular is able to correctly identify the presence of rip currents in all 8 of the videos.

VI. IMPLEMENTATION NOTES

We implemented the methods above with C++ along with OpenCV library. We used Alienware m3 R15 with RTX 2070 Super for computation, and it consumes roughly 1GB of memory. We used GPU acceleration mainly for optical flow computation, and with a dedicated GPU, our method ran in real-time with 30 FPS on 1080×720 resolution.

VII. SUMMARY AND CONCLUSION

We investigated rip current detection using optical flow analysis on video clips. This is complicated because rip currents are amorphous without well defined boundaries and ephemeral without well defined temporal bounds. The problem is further complicated by the presence of a dominant quasi-periodic signal from wave motion. We found that the straight-forward application of flow visualization methods did not yield good results. The main contributions of this paper are the modifications to standard flow visualization methods in order to equip them with rip current detection capability without which the detection is difficult or impossible. The modifications significantly improved upon earlier flow based method both in terms of ability to detect subtle rips and clarity in visualization. Our study also shows that our proposed flow based visualization results in improved human judgements versus the existing dominant method of viewing Timex images.

Flow-based approach is a valuable tool to have in our arsenal of rip detection methods. It is best suited for situations where a stable platform for a camera is available e.g. surf cams. In such settings, site specific customizations e.g. placement of timelines can be employed to make the approach fully automated. The work presented here has shown sufficient success that it will be deployed on the SECOORA network of webcams.

APPENDIX

Our code is available in the following GitHub repository. https://github.com/IsseiMori/Flow-based-Rip-Current-Detection

ACKNOWLEDGMENT

The authors thank Ra'Teema Stanley for labeling the data from Miami beach webcams. The statements, findings, conclusions, and recommendations are those of the author(s) and do not necessarily reflect the views of SECOORA or NOAA.

REFERENCES

[1] B. Brighton, S. Sherker, R. Brander, M. Thompson, and A. Bradstreet, "Rip current related drowning deaths and rescues in Australia 2004-2011," *Natural Hazards Earth Syst. Sci.*, vol. 13, pp. 1069–1075, Apr. 2013.

[2] A. H. F. da Klein, G. G. Santana, F. L. Diehl, and J. T. de Menezes, "Analysis of hazards associated with sea bathing: Results of five years work in oceanic beaches of Santa Catarina state, Southern Brazil," *J. Coastal Res.*, vol. 35, pp. 107–116, Apr. 2003. [Online]. Available: http://www.jstor.org/stable/40928754

[3] J. B. Lushine, "A study of rip current drownings and related weather factors," *Nat. Weather Dig.*, vol. 16, no. 3, pp. 13–19, Aug. 1991.

[4] B. C. Brewster, R. E. Gould, and R. W. Brander, "Estimations of rip current rescues and drowning in the United States," *Natural Hazards Earth Syst. Sci.*, vol. 19, no. 2, pp. 389–397, Feb. 2019.

[5] N. Oceanic and A. Administration. (2020). *Safety National Program Surf Zone Fatalities in NWS Areas of Forecast Responsibility*. [Online]. Available: https://www.weather.gov/safety/ripcurrent-fatalities

[6] S. L. J. Fletemeyer, "Rip currents and beach safety education," *J. Coastal Res.*, vol. 26, no. 1, pp. 1–3, Jan. 2010.

[7] R. W. Brander and J. H. MacMahan, "Future challenges for rip current research and outreach," in *Rip Currents: Beach Safety, Physical Oceanography, and Wave Modeling*, S. Leatherman and J. Fletemeyer, Eds. Boca Raton, FL, USA: CRC Press, 2011, pp. 1–30.

[8] C. Brannstrom, S. Trimble, A. Santos, H. L. Brown, and C. Houser, "Perception of the rip current hazard on Galveston island and north padre island, Texas, USA," *Natural Hazards*, vol. 72, no. 2, pp. 1123–1138, Jun. 2014.

[9] C. Houser, S. Trimble, R. Brander, B. C. Brewster, G. Dusek, D. Jones, and J. Kuhn, "Public perceptions of a rip current hazard education program: 'Break the grip of the rip,'" *Natural Hazards Earth Syst. Sci.*, vol. 17, no. 7, pp. 1003–1024, Jul. 2017.

[10] A. J. Bowen, "Rip currents: 1. theoretical investigations," *J. Geophys. Res.*, vol. 74, no. 23, pp. 5467–5478, Oct. 1969.

[11] R. A. Holman, G. Symonds, E. B. Thornton, and R. Ranasinghe, "Rip spacing and persistence on an embayed beach," *J. Geophys. Res.*, vol. 111, no. C1, pp. 1–17, 2006.

[12] B. Castelle, T. Scott, R. W. Brander, and R. J. McCarroll, "Rip current types, circulation and hazard," *Earth-Sci. Rev.*, vol. 163, pp. 1–21, Dec. 2016.

[13] G. Dusek and H. Seim, "A probabilistic rip current forecast model," *J. Coastal Res.*, vol. 289, pp. 909–925, Jul. 2013.

[14] L. Sembiring, "Rip current prediction system for swimmer safety: Towards operational forecasting using a process based model and nearshore bathymetry from video," TU Delft, The Netherlands, Tech. Rep., 2016, doi: 10.4233/uuid:9185f607-ad49-4ac5-b218-3eaa4642d544.

[15] *NOAA Launches First National Rip Current Forecast Model*. Accessed: Apr. 7, 2021. [Online]. Available: https://oceanservice.noaa.gov/news/apr21/rip-current-forecast.html

[16] S. L. S. Australia (2019). *National Coastal Safety Report*. [Online]. Available: https://issuu.com/surflifesavingaustralia/docs/ncsr2019

[17] C. M. Branche, "Lifeguard effectiveness: A report of the working group," in *National Center for Injury Prevention and the Centers for Disease Control and Prevention*. Atlanta, GA, USA, 2001. [Online]. Available: https://www.cdc.gov/homeandrecreationalsafety/pubs/lifeguardreport-a.pd%f

[18] C. Brannstrom, H. Lee Brown, C. Houser, S. Trimble, and A. Santos, "'You can't see them from sitting here': Evaluating beach user understanding of a rip current warning sign," *Appl. Geography*, vol. 56, pp. 61–70, Jan. 2015.

[19] S. B. Leatherman and S. P. Leatherman, "Techniques for detecting and measuring rip currents," *Int. J. Earth Sci. Geophys.*, vol. 3, no. 1, pp. 1–5, Dec. 2017.

[20] S. Elgar, B. Raubenheimer, and R. T. Guza, "Current meter performance in the surf zone," *J. Atmos. Ocean. Technol.*, vol. 18, no. 10, pp. 1735–1746, Oct. 2001.

[21] K. Inch, "Surf zone hydrodynamics: Measuring waves and currents," *Geomorpholog. Techn.*, vol. 3, pp. 1–13, Jun. 2014.

[22] D. Johnson, "Transient rip currents and nearshore circulation on a swell-dominated beach," *J. Geophys. Res.*, vol. 109, no. C2, 2004, Art. no. C02026, doi: 10.1029/2003JC001798.

[23] Y. Liu and C. H. Wu, "Lifeguarding operational camera kiosk system (LOCKS) for flash rip warning: Development and application," *Coastal Eng.*, vol. 152, Oct. 2019, Art. no. 103537.

[24] R. W. Brander, D. Drozdzewski, and D. Dominey-Howes, "'Dye in the water': A visual approach to communicating the rip current hazard," *Sci. Commun.*, vol. 36, no. 6, pp. 802–810, 2014.

[25] D. B. Clark, F. Feddersen, and R. T. Guza, "Cross-shore surfzone tracer dispersion in an alongshore current," *J. Geophys. Res., Oceans*, vol. 115, no. C10, Oct. 2010, Art. no. C10035.

[26] D. B. Clark, L. Lenain, F. Feddersen, E. Boss, and R. T. Guza, "Aerial imaging of fluorescent dye in the near shore," *J. Atmos. Ocean. Technol.*, vol. 31, no. 6, pp. 1410–1421, Jun. 2014.

[27] D. W. Pritchard and J. H. Carpenter, "Measurements of turbulent diffusion in estuarine and inshore waters," *Int. Assoc. Sci. Hydrol. Bull.*, vol. 5, no. 4, pp. 37–50, Dec. 1960, doi: 10.1080/02626666009493189.

[28] B. Castelle, R. Almar, M. Dorel, J.-P. Lefebvre, N. Senechal, E. J. Anthony, R. Laibi, R. Chuchla, and Y. du Penhoat, "Rip currents and circulation on a high-energy low-tide-terraced beach (Grand Popo, Benin, West Africa)," *J. Coastal Res.*, vol. 70, pp. 633–638, Apr. 2014, doi: 10.2112/SI70-107.1.

[29] W. E. Schmidt, B. T. Woodward, K. S. Millikan, R. T. Guza, B. Raubenheimer, and S. Elgar, "A GPS-tracked surf zone drifter," *J. Atmos. Ocean. Technol.*, vol. 20, no. 7, pp. 1069–1075, Jul. 2003.

[30] G. Dusek, D. Hernandez, M. Willis, J. A. Brown, J. W. Long, D. E. Porter, and T. C. Vance, "WebCAT: Piloting the development of a web camera coastal observing network for diverse applications," *Frontiers Mar. Sci.*, vol. 6, p. 353, Jun. 2019.

[31] K. T. Holland, R. A. Holman, T. C. Lippmann, J. Stanley, and N. Plant, "Practical use of video imagery in nearshore oceanographic field studies," *IEEE J. Ocean. Eng.*, vol. 22, no. 1, pp. 81–92, Jan. 1997.

[32] R. A. Holman and J. Stanley, "The history and technical capabilities of Argus," *Coast. Eng.*, vol. 54, no. 6, pp. 477–491, Jun./Jul. 2007.

[33] T. C. Lippmann and R. A. Holman, "Quantification of sand bar morphology: A video technique based on wave dissipation," *J. Geophys. Res., Oceans*, vol. 94, no. C1, pp. 995–1011, 1989.

[34] S. Pitman, S. L. Gallop, I. D. Haigh, S. Mahmoodi, G. Masselink, and R. Ranasinghe, "Synthetic imagery for the automated detection of rip currents," *J. Coastal Res.*, vol. 75, no. 1, pp. 912–916, Mar. 2016.

[35] C. Maryan, M. T. Hoque, C. Michael, E. Ioup, and M. Abdelguerfi, "Machine learning applications in detecting rip channels from images," *Appl. Soft Comput.*, vol. 78, pp. 84–93, May 2019.

[36] V. Nelko and R. Dalrymple, "Rip current prediction in ocean city, Maryland," in *Rip Currents: Beach Safety, Physical Oceanography and Wave Modeling*. Boca Raton, FL, USA: CRC Press, 2011, pp. 45–58. [Online]. Available: https://www.academia.edu/1017360/Rip_Current_Prediction_at_Ocean_City_M%aryland

[37] A. de Silva, I. Mori, G. Dusek, J. Davis, and A. Pang, "Automated rip current detection with region based convolutional neural networks," *Coastal Eng.*, vol. 166, Jun. 2021, Art. no. 103859. [Online]. Available: https://www.sciencedirect.com/science/article/pii/S0378383921000193

[38] J. L. Barron, D. J. Fleet, and S. S. Beauchemin, "Performance of optical flow techniques," *Int. J. Comput. Vis.*, vol. 12, no. 1, pp. 43–77, 1994, doi: 10.1007/BF01420984.

[39] B. K. P. Horn and B. G. Schunck, "Determining optical flow," *Artif. Intell.*, vol. 17, nos. 1–3, pp. 185–203, Aug. 1980, doi: 10.1016/0004-3702(81)90024-2.

[40] P. Derian and R. Almar, "Wavelet-based optical flow estimation of instant surface currents from shore-based and UAV videos," *IEEE Trans. Geosci. Remote Sens.*, vol. 55, no. 10, pp. 5790–5797, Oct. 2017.

[41] S. Philip and A. Pang, "Detecting and visualizing rip current using optical flow," in *Proc. Eurographics, EuroVis*. Goslar Germany, Germany: Eurographics Association, 2016, pp. 19–23.

[42] D. Anderson, A. S. Bak, K. L. Brodie, N. Cohn, R. A. Holman, and J. Stanley, "Quantifying optically derived two-dimensional wave-averaged currents in the surf zone," *Remote Sens.*, vol. 13, no. 4, p. 690, Feb. 2021. [Online]. Available: https://www.mdpi.com/2072-4292/13/4/690

[43] F. Liu, M. Gleicher, J. Wang, H. Jin, and A. Agarwala, "Subspace video stabilization," *ACM Trans. Graph.*, vol. 30, no. 1, pp. 1–10, Jan. 2011.

[44] Y. Matsushita, E. Ofek, W. Ge, X. Tang, and H.-Y. Shum, "Full-frame video stabilization with motion inpainting," *IEEE Trans. Pattern Anal. Mach. Intell.*, vol. 28, no. 7, pp. 1150–1163, Jul. 2006.

[45] B. Zitová and J. Flusser, "Image registration methods: A survey," *Image Vis. Comput.*, vol. 21, pp. 977–1000, Oct. 2003.
[46] L. G. Brown, "A survey of image registration techniques," *ACM Comput. Surv.*, vol. 24, no. 4, pp. 325–376, Dec. 1992.
[47] G. Farneback, "Two-frame motion estimation based on polynomial expansion," *Scandin. Conf. Image Anal.*, vol. 13, pp. 363–370, Jun. 2003.
[48] B. Lucas and T. Kanade, "An iterative image registration technique with an application to stereo vision," in *Proc. Int. Joint Conf. Artif. Intell.*, 1981, pp. 674–679.
[49] S. Baker and I. Matthews, "Lucas-Kanade 20 years on: A unifying framework," *Int. J. Comput. Vis.*, vol. 56, no. 3, pp. 221–255, 2004.
[50] S. S. Beauchemin and J. L. Barron, "The computation of optical flow," *ACM Comput. Surv.*, vol. 27, no. 3, pp. 433–466, Sep. 1995.
[51] B. Gary and A. Kaehle, "OpenCV," *Dr. Dobb's J. Softw. Tools*, vol. 25, no. 11, pp. 122–125, 2000.
[52] D. A. Lane, "Visualization of time-dependent flow fields," in *Proc. Visualizat.*, Oct. 1993, pp. 32–38.
[53] S. C. O. O. R. A. Secoora. (2020). *Webcat Live Cameras and Historic Feeds*. [Online]. Available: https://secoora.org/webcat/
[54] P. Viola and M. Jones, "Rapid object detection using a boosted cascade of simple features," in *Proc. IEEE Comput. Soc. Conf. Comput. Vis. Pattern Recognit. (CVPR)*, Dec. 2001, p. 3.
[55] S. Ren, K. He, R. Girshick, and J. Sun, "Faster R-CNN: Towards real-time object detection with region proposal networks," in *Proc. Adv. Neural Inf. Process. Syst.*, C. Cortes, N. D. Lawrence, D. D. Lee, M. Sugiyama, and R. Garnett, Eds. Cambridge, MA, USA: MIT Press, 2015, pp. 91–99.

ISSEI MORI is currently pursuing the B.S. degree in computer science with the University of California at Santa Cruz. His research interests include computer vision, 3D geometry, and graphics rendering.

AKILA DE SILVA received the B.S. degree from the Asian Institute of Technology, Thailand, and the M.S. degree from Columbia University, City of New York. He is currently pursuing the Ph.D. degree in computer science with the University of California at Santa Cruz. His research interests include computer vision, machine learning, and flow visualization.

GREGORY DUSEK received the B.S. degree in applied mathematics and the M.S. degree in teaching and curriculum from the University of Rochester, Rochester, NY, USA, in 2004 and 2005, respectively, and the Ph.D. degree in marine science from the University of North Carolina at Chapel Hill, Chapel Hill, NC, USA, in 2011. Since 2014, he has been the Chief Scientist with the NOAA National Ocean Service, Center for Operational Oceanographic Products and Services. He is currently a Physical Oceanographer.

JAMES DAVIS (Senior Member, IEEE) received the Ph.D. degree from Stanford University, in 2002. From 2002 to 2004, he was a Senior Research Scientist at Honda Research Institute. He is currently a Professor of computer science engineering at the University of California at Santa Cruz. His research interests include both traditional computer science and technology applications to social issues. This work has resulted in over 100 peer-reviewed publications, patents, and invited talks, received an IEEE ICRA 2003 Best Vision Paper, IEEE ICCV 2009 Marr Prize, and an NSF CAREER Award. His teaching has twice been awarded for innovative style, including a course on the importance of technology to social entrepreneurship. He is on the advisory boards of several for-profit and non-profit organizations, and co-founded Bellus3D, in 2015.

ALEX PANG is currently a Professor of computer science and engineering at the UC Santa Cruz. His research interests include comparative and uncertainty visualization, flow and tensor visualization, and applications for social good.